Inorg. Chem. **2006**, *45*, 3732–3740

Mechanistic Analysis of the Electrocatalytic Properties of Dissolved α and β Isomers of $[SiW_{12}O_{40}]^{4-}$ and Solid $[Ru(bipy)_3]_2[\alpha\text{-}SiW_{12}O_{40}]$ on the Reduction of Nitrite in Acidic Aqueous Media

Jie Zhang,[†] Joo-Kheng Goh,[‡] Wee-Tee Tan,[§] and Alan M. Bond*,[†]

School of Chemistry, Monash University, Clayton, Victoria 3800, Australia, School of Arts and Sciences, Monash University Malaysia, 46150 Petaling Jaya, Selangor Darul Ehsan, and Department of Chemistry, Faculty of Science, Universiti Putra Malaysia, 43400 Serdang, Selangor Darul Ehsan

Received November 17, 2005

Voltammetric studies on the reduction of α and β isomers of the Keggin polyoxometalate anion $[SiW_{12}O_{40}]^{4-}$ reveal a series of electrochemically reversible processes in acidic aqueous media. In the presence of NO_2^-, catalytic current is detected in the potential region of the $[SiW_{12}O_{40}]^{4-/5-}$ process. Electronic spectroscopy and simulation of voltammetric data undertaken at variable $[NO_2^-]$ and $[H^+]$ allow the following mechanism to be postulated, $[SiW_{12}O_{40}]^{4-} + e^- \rightleftharpoons [SiW_{12}O_{40}]^{5-}$, $H^+ + HNO_2 \rightleftharpoons NO^+ + H_2O$, $NO^+ + [SiW_{12}O_{40}]^{5-} \rightarrow NO + [SiW_{12}O_{40}]^{4-}$. The second-order rate constant for the rate-determining step is faster for the α isomer than for the β one. This may be attributed to the different reversible potentials of –0.144 V (α isomer) and –0.036 V vs Ag/AgCl (β isomer) and, hence, smaller driving force for an assumed outer sphere electron-transfer reaction in the case of β isomer. A stable, water-insoluble, thin-film $[Ru(bipy)_3]_2[\alpha\text{-}SiW_{12}O_{40}]$ chemically modified electrode was generated electrochemically via ion-exchange of $[Ru(bipy)_3]^{2+}$ with Bu_4N^+ in the $[Bu_4N]_4[\alpha\text{-}SiW_{12}O_{40}]$ solid. The first reduction process with this modified electrode gives rise to the reaction $[Ru(bipy)_3]_2[\alpha\text{-}SiW_{12}O_{40}]$(solid) + H^+(soln) + $e^- \rightleftharpoons H[Ru(bipy)_3]_2[\alpha\text{-}SiW_{12}O_{40}]$(solid). The need to transfer a proton from the solution to the solid phase for charge neutralization purposes introduces a hydrogen-ion concentration dependence into this reaction, which is not found in the solution-phase study. Nevertheless, the voltammetric catalytic activity with respect to nitrite reduction is retained with the chemically modified electrode. However, nitrite catalysis with the $[Ru(bipy)_3]_2[\alpha\text{-}SiW_{12}O_{40}]$-modified electrode is now independent of concentration of H^+, rather than exhibiting a first-order dependence, and full mechanistic details for this process are unknown.

Introduction

There is a long history of polyoxometalate chemistry.[1] For example, $(NH_4)_3[PMo_{12}O_{40}]$ was synthesized in 1826[2] and the structure of $H_3PW_{12}O_{40}\cdot 5H_2O$ was determined by Keggin in 1934 using X-ray diffraction.[3] Polyoxometalates with related structures are called Keggin-type clusters.

Electrochemical studies involving polyoxometalate anions frequently contain examples of electrocatalytic reaction schemes.[4−11] For example, the pioneering work by Toth and Anson[8] has shown that the reduced forms of iron-substitute polyoxotungstates, $[Fe(III)XW_{11}O_{39}]^{n-}$ (X = Si or Ge, n = 5; X = As or P, n = 4) can catalyze nitrite reduction to

* To whom correspondence should be addressed. E-mail: alan.bond@sci.monash.edu.au.
[†] Monash University.
[‡] Monash University Malaysia.
[§] Universiti Putra Malaysia.

(1) Pope, M. T. *Heteropoly and Isopoly Oxometalates*; Springer-Verlag: Berlin, 1983.
(2) Berzelius, J. *Pogg. Ann.* **1826**, *6*, 369, 380.
(3) Keggin, J. F. *Nature* **1933**, *131*, 908.
(4) Sadakane, M.; Steckhan, E. *Chem. Rev.* **1998**, *98*, 219.
(5) Bond, A. M. *Broadening Electrochemical Horizons: Principles and Illustration of Voltammetric and Related Techniques*; Oxford University Press: Oxford, 2002.
(6) Moffat, J. B. *Metal−Oxygen Clusters: The Surface and Catalytic Properties of Heteropoly Oxometalates*; Kluwer Academic/Plenum Publisher: New York, 2001.
(7) Keita, B.; Nadjo, L.; Haeussler, J. P. *J. Electroanal. Chem.* **1987**, *230*, 85.
(8) Toth, J. E.; Anson, F. C. *J. Am. Chem. Soc.* **1989**, *111*, 2444.
(9) Toth, J. E.; Melton, J. D.; Cabelli, D.; Bielski, B. H. J.; Anson, F. C. *Inorg. Chem.* **1990**, *29*, 1952.
(10) Dong, S.; Liu, M. *J. Electroanal. Chem.* **1994**, *372*, 95.
(11) Dong, S.; Xi, X.; Tian, M. *J. Electroanal. Chem.* **1995**, *385*, 227.

10.1021/ic0519943 CCC: $33.50
Published on Web 04/01/2006

ammonia at pH 2−8. Subsequently, Dong and co-workers[11] showed that catalytic reaction between reduced $[\alpha\text{-}SiW_{12}O_{40}]^{4-}$ and nitrite is detectable voltammetrically when the aqueous media is sufficiently acidic. The electrocatalytic properties of $[\alpha\text{-}SiMo_{12}O_{40}]^{4-}$ toward nitrite also has been investigated by Nadjo and co-workers.[12] Since the determination of nitrite is biologically, environmentally, and industrially important,[13] electrodes chemically modified with Keggin-type and other types of polyoxometalate anions have been developed for this purpose.[12,14]

Despite an extensive amount of literature on the subject, quantitative accounts of the kinetics and mechanistic insights related to the origin of unsubstituted polyoxometalate catalytic activity toward nitrite reduction, in both dissolved and surface confined states, are relatively rare.[11] In this paper, the catalytic reduction of nitrite with electrogenerated reduced forms of α and *β* isomers of $[SiW_{12}O_{40}]^{4-}$ is described under both conventional conditions with dissolved polyoxometalate and also using electrodes that are modified with a $[Ru(bipy)_3]_2[\alpha\text{-}SiW_{12}O_{40}]$ film. The rate constants for electrocatalytic reactions with dissolved α and *β* isomers of $[SiW_{12}O_{40}]^{4-}$ are deduced by quantitative analysis of the proposed reaction scheme. UV−visible spectroelectrochemical data are also presented to support the postulated mechanism.

Experimental Section

Materials and Reagents. $K_4[\alpha\text{-}SiW_{12}O_{40}]$, $K_4[\beta\text{-}SiW_{12}O_{40}]$, and $[Bu_4N]_4[\alpha\text{-}SiW_{12}O_{40}]$ were synthesized according to literature procedures.[15,16] Tris(2,2′-bipyridyl)dichlororuthenium(II) hexahydrate was purchased from Aldrich. Other chemicals and organic solvents (BDH) were of analytical reagent grade and used as received from the manufacturer. Deionized distilled water was used for the preparation of aqueous solutions.

Instrumentation and Procedures. Voltammetric, rotating disk electrode (RDE), and bulk electrolysis experiments were undertaken with a BAS 100 B (Bioanalytical Systems, West Lafayette, IN) electrochemical workstation. A 3-mm-diameter glassy carbon disk electrode (GC) working electrode, a platinum wire (1 mm diameter) counter electrode, and an Ag/AgCl (3M KCl) reference electrode were used in voltammetric and RDE experiments. The working electrodes were polished with a 0.3-*μ*m alumina slurry before use. For bulk electrolysis experiments, a BAS GC gauze electrode was used as the working electrode along with a Pt gauze counter electrode (present in a salt bridge containing electrolyte solution but separated from the bulk solution) and a Ag/AgCl (saturated KCl) reference electrode. All solutions were degassed with nitrogen prior to undertaking electrochemical measurements. A Cary 15 UV−vis NIR spectrophotometer (Varian) was used to obtain electronic spectra.

DigiSim software (version 3.1)[17] was used to simulate cyclic voltammetric responses.

Preparation of a $[Ru(bipy)_3]_2[\alpha\text{-}SiW_{12}O_{40}]$-Modified Electrode. Unless otherwise specified, 1 *μ*L of a 0.4 mM acetonitrile solution of $[Bu_4N]_4[\alpha\text{-}SiW_{12}O_{40}]$ was transferred to the surface of a GC electrode using a microsyringe. On drying in air, a film containing an array of $[Bu_4N]_4[\alpha\text{-}SiW_{12}O_{40}]$ microcrystals was formed on the electrode surface. This chemically modified electrode was then immersed in a 5 mM $[Ru(bipy)_3]^{2+}$ solution containing 0.2 M Na_2SO_4 electrolyte. Finally, the potential of the electrode was cycled over the range of +0.6 to −1.1 V (three cycles). At negative potential, reduction of $[Bu_4N]_4[\alpha\text{-}SiW_{12}O_{40}]$ microcrystals initially leads to uptake of Na^+ ions in order to achieve charge neutrality in the solid phase.[18] These water-soluble reduced forms of $[\alpha\text{-}SiW_{12}O_{40}]^{4-}$ then reprecipitate in the presence of $[Ru(bipy)_3]^{2+}$ to produce stable, water-insoluble films. Alternatively, chemically modified electrodes of this type can also be fabricated by direct coating with a solution of $[Ru(bipy)_3]_2[\alpha\text{-}SiW_{12}O_{40}]$[19] or by a layer-by-layer assembly method as described by Dong and co-workers.[20]

Results and Discussion

1. Catalytic Behavior of Nitrite when Dissolved α and *β* Isomers of $[SiW_{12}O_{40}]^{4-}$ are Voltammetrically Reduced at an Electrode. 1.1. Solution-Phase Voltammetry of $[\alpha\text{-}SiW_{12}O_{40}]^{4-}$ in Acidic Media. The voltammetry of $[\alpha\text{-}SiW_{12}O_{40}]^{4-}$ dissolved in 0.01, 0.1, and 1.0 M sulfuric acid media containing 1 M Na_2SO_4 enables the effect of the hydrogen ion concentration to be established.

Voltammograms of $[\alpha\text{-}SiW_{12}O_{40}]^{4-}$ consist of three well-separated reduction processes in sulfuric acid media. The voltammetric characteristics of the first two processes (labeled I and II in Figure 1a) are almost independent of pH, in agreement with data reported previously.[14c,21] The peak-to-peak separation, ΔE_p, of ca. 59 mV between the reduction, E^p_{red}, and oxidation, E^p_{ox}, peak potentials (scan rate of 0.1 V s^{-1}) is close to the theoretical value of 56 mV expected for a reversible one-electron transfer process at 20 °C[22] (the slightly larger peak separation than the theoretically predicted value is attributed to the presence of a small level of uncompensated resistance). The magnitude of the peak current for the third process (labeled III in Figure 1a) is significantly larger than for the one-electron processes I and II, and the ΔE_p, of ca. 37 mV for this process is close to half of those for processes I and II. Furthermore, in this case, the reversible potential ($E^{0'}_{soln}$, calculated as $(E^p_{red} + E^p_{ox})/2$) for process III shifts by about 105 mV per decade change in proton concentration (range of 0.01−1.0 M H_2SO_4), as reported in other highly acidic aqueous media;[11,23] thus, this dependence on pH corresponds to an overall two-electron, four-proton process. The number of protons accompanying the two-electron transfer process was not estimated in

(12) Keita, B.; Belhouari, A.; Nadjo, L.; Contant, R. *J. Electroanal. Chem.***1995**, *381*, 243.
(13) Moorcroft, M. J.; Davis, J.; Compton, R. G. *Talanta* **2001**, *54*, 785.
(14) (a) Fay, N.; Dempsy, E.; McCormac, T. *J. Electroanal. Chem.* **2005**, *574*, 359. (b) McCormac, T.; Farrell, D.; Drennan, D.; Biden, G. *Electroanalysis* **2001**, *13*, 836. (c) Cheng, L.; Liu, J.; Dong, S. *Anal. Chim. Acta* **2000**, *417*, 133. (d) Liu, S.; Shi, Z.; Dong, S. *Electroanalysis* **1998**, *10*, 891. (e) Rong, C.; Anson, F. C. *Inorg. Chim. Acta* **1996**, *242*, 11. (f) Kulesza, P. J.; Roslonek, G.; Faulkner, L. R. *J. Electroanal. Chem.* **1990**, *280*, 233.
(15) Tézé, A.; Hervé, G. *Inorg. Synth.* **1990**, *27*, 85.
(16) Rocchiccioli-Deltcheff, C.; Fournier, M.; Franck, R.; Thouvenot, R. *Inorg. Chem.* **1983**, *22*, 207.
(17) Rudolph, M.; Reddy, D. P.; Feldberg, S. W. *Anal. Chem.* **1994**, *66*, 589A.
(18) Zhang, J.; Bond, A. M. *J. Electroanal. Chem.* **2005**, *574*, 299.
(19) Hultgren, V. M.; Bond, A. M.; Wedd, A. G. *J. Chem. Soc., Dalton Trans.* **2001**, 1076.
(20) Bi, L.; Wang, H.; Shen, Y.; Wang, E.; Dong, S. *Electrochem. Commun.* **2003**, *5*, 913.
(21) Pope, M. T.; Varga, G. M., Jr. *Inorg. Chem.* **1966**, *5*, 1249.
(22) Oldham, K. B.; Myland, J. C. *Fundamentals of Electrochemical Science*; Academic Press: San Diego, 1994.

Table 1. Reversible Potentials (vs Ag/AgCl) and Other Voltammetric Data of $[\alpha\text{-SiW}_{12}O_{40}]^{4-}$ Reduction at a 3-mm-Diameter GC Electrode at Different Concentrations of H_2SO_4 ($\upsilon = 0.1$ V s^{-1})

	Process I				Process II				Process III			
$c_{H_2SO_4}$/M	E^p_{red}/V	E^p_{ox}/ V	ΔE_p/V	$E^{0'}_{soln}$/V	E^p_{red}/V	E^p_{ox}/V	ΔE_p/V	$E^{0'}_{soln}$/V	E^p_{red}/V	E^p_{ox}/V	ΔE_p/V	$E^{0'}_{soln}$/V
0.010	−0.176	−0.118	0.058	−0.147	−0.434	−0.375	0.059	−0.405	−0.800	−0.762	0.038	−0.781
0.10	−0.169	−0.110	0.059	−0.140	−0.422	−0.363	0.059	−0.393	−0.703	−0.664	0.037	−0.684
1.0	−0.169	−0.110	0.059	−0.140	−0.398	−0.340	0.058	−0.369	−0.587	−0.551	0.036	−0.569

previous studies at low pH. In the higher pH range, a two-electron, two-proton mechanism is assigned to the third process.[14c] Mechanisms involving proton transfer coupled to reduction of polyoxometalates are often very complicated and may strongly depend on the acidity of the media.[24] The reversible potentials and other voltammetric data obtained at different concentrations of H_2SO_4 ($c_{H_2SO_4}$) are given in Table 1. In summary, the reactions associated with reduction of $[\alpha\text{-SiW}_{12}O_{40}]^{4-}$ in concentrated H_2SO_4 are represented by eq 1

$$[\alpha\text{-SiW}_{12}O_{40}]^{4-} \underset{-e^-}{\overset{+e^-}{\rightleftharpoons}} [\alpha\text{-SiW}_{12}O_{40}]^{5-} \underset{-e^-}{\overset{+e^-}{\rightleftharpoons}} [\alpha\text{-SiW}_{12}O_{40}]^{6-} \underset{-2e^- -4H^+}{\overset{+2e^- +4H^+}{\rightleftharpoons}} [\alpha\text{-H}_2\text{SiW}_{12}O_{40}]^{6-} \quad (1)$$

The catalytic process of interest in this study is associated with process I. Over all scan rates and acidities examined, the $E^{0'}_{soln}$ value for this $[\alpha\text{-SiW}_{12}O_{40}]^{4-/5-}$ process is -0.144 ± 0.005 V vs Ag/AgCl. Figure 1b provides a comparison of an experimental voltammogram and one simulated assuming reversible conditions are applicable (very large value of the heterogeneous electron-transfer rate constant at $E^{0'}_{soln}$) for process I in 1 M H_2SO_4 + 1 M Na_2SO_4. Excellent agreement can be noted. A diffusion coefficient (D) of 3.7×10^{-6} cm^2 s^{-1} is obtained from this theory−experiment comparison, which is close to the value of 3.65×10^{-6} cm^2 s^{-1} reported in 0.5 M H_2SO_4.[11]

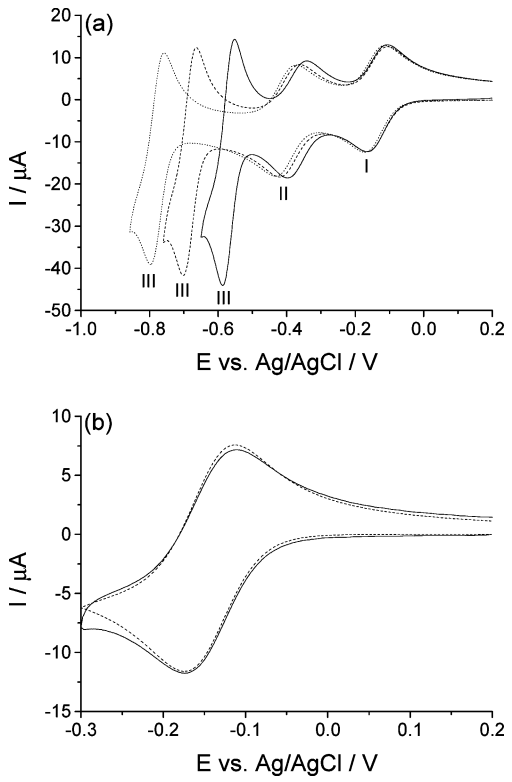

Figure 1. Cyclic voltammograms obtained at a scan rate of 0.1 V s^{-1} for reduction of 1 mM $[\alpha\text{-SiW}_{12}O_{40}]^{4-}$ at a 3-mm-diameter GC electrode. (a) All three processes in 0.01 (···), 0.1 (- - -), and 1 M (—) H_2SO_4 containing 1 M Na_2SO_4. (b) Comparison of the experimental voltammogram (—) for the first process in 1 M H_2SO_4 + 1 M Na_2SO_4 and simulated (- - -) data obtained for a reversible one-electron reduction process with $D = 3.7 \times 10^{-6}$ cm^2 s^{-1} and $E^{0'}_{soln} = -0.144$ V vs Ag/AgCl.

1.2. Catalytic Effect in the Presence of Nitrite. It is well-known that HNO_2 can disproportionate to form NO and NO_3^-,[25]

$$3HNO_2 \rightarrow H^+ + 2NO + NO_3^- + H_2O \quad (2)$$

To ensure that the influence of this reaction is minimal, experimental data relevant to nitrite catalysis were always obtained from freshly prepared solutions.

Cyclic voltammograms contained in Figure 2 show that the magnitude of the $[\alpha\text{-SiW}_{12}O_{40}]^{4-/5-}$ reduction current is significantly enhanced in the presence of NO_2^-, under low-pH conditions (Figure 2a,b). However, the magnitude of current enhancement decreases as the pH increases (Figure 2c), even though the reversible potential of the $[\alpha\text{-SiW}_{12}O_{40}]^{4-/5-}$ process is essentially independent of pH. The fact that the pH values used in this study are all lower than the pK_a value of HNO_2 (3.3 at 18 °C[25]), suggests that $[\alpha\text{-SiW}_{12}O_{40}]^{5-}$ catalyzes the reduction of HNO_2 (≥90% of nitrite is in the acidic form at pH values studied), rather than NO_2^-. Clearly, the mechanism for the catalytic activity of $[\alpha\text{-SiW}_{12}O_{40}]^{5-}$ differs from that with $[Fe(II)GeW_{11}O_{39}]^{6-}$ and NO_2^- where the apparent second-order catalytic rate constant is proportional to the proton concentration over the pH range of 4−8 but essentially independent of pH when pH ≤ pK_a of HNO_2.[8]

1.3. Rotating Disk Electrode Voltammetry and UV−Visible Spectrophotometery. Electronic spectra of $[\alpha\text{-SiW}_{12}O_{40}]^{4-}$ in aqueous 1 M H_2SO_4 + 1 M Na_2SO_4 electrolyte are identical in the presence and absence of NO_2^-, which suggests no complex is formed between them. A bulk one-electron reductive electrolysis of colorless $[\alpha\text{-SiW}_{12}O_{40}]^{4-}$ in this medium produces a blue solution. Monitoring the course of this electrolysis by RDE voltammetry reveals that the transition in process I from fully reductive ($[\alpha\text{-SiW}_{12}O_{40}]^{4-/5-}$ process) to fully oxidative ($[\alpha\text{-SiW}_{12}O_{40}]^{5-/4-}$ process) occurs, as expected if $[\alpha\text{-SiW}_{12}O_{40}]^{4-}$ is completely converted to $[\alpha\text{-SiW}_{12}O_{40}]^{5-}$. Addition of an equimolar concentration of NO_2^- leads to the immediate

(23) Keita, B.; Nadjo, L. *J. Electroanal. Chem.* **1987**, *217*, 287.
(24) Guo S. X.; Feldberg, S. W.; Bond, A. M.; Callahan, D. L.; Richardt, P. J. S.; Wedd, A. G. *J. Phys. Chem. B* **2005**, *109*, 20641.
(25) Jolly, W. L. *Inorganic Chemistry of Nitrogen*; W. A. Benjamin: New York, 1964.

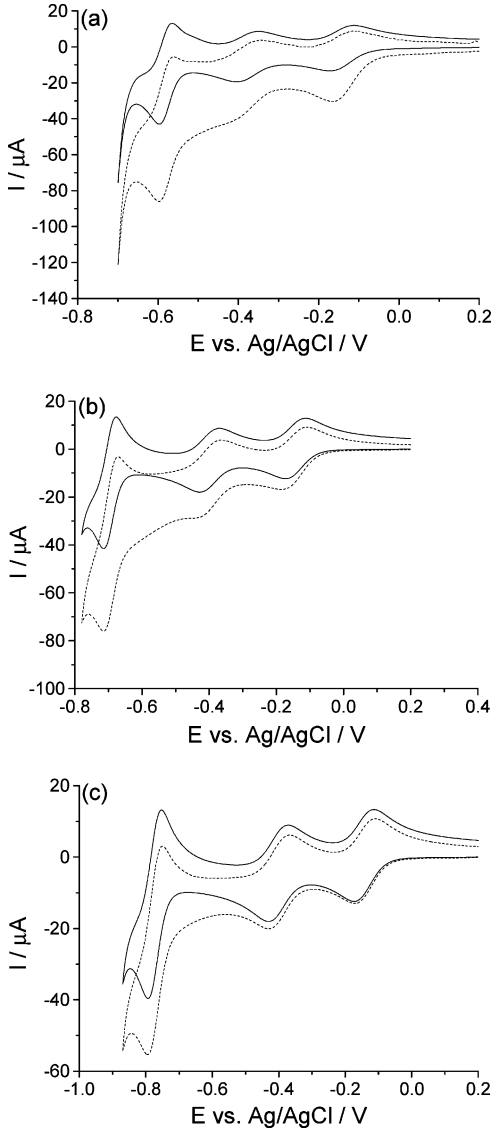

Figure 2. Cyclic voltammograms obtained at a scan rate of 0.1 V s^{-1} for reduction of 0.9 mM $[\alpha\text{-}SiW_{12}O_{40}]^{4-}$ at a 3-mm-diameter GC electrode in the absence (—) and presence (- - -) of 0.8 mM NO_2^- in the aqueous media containing 1 M Na_2SO_4 together with (a) 1, (b) 0.1, and (c) 0.01 M H_2SO_4.

disappearance of the blue color and full recovery of the RDE voltammogram to the original state. This is as expected if $[\alpha\text{-}SiW_{12}O_{40}]^{5-}$ is oxidized by HNO_2 in sulfuric acid media to reform $[\alpha\text{-}SiW_{12}O_{40}]^{4-}$, according to eq 3.

$$H^+ + HNO_2 + [\alpha\text{-}SiW_{12}O_{40}]^{5-} \rightarrow NO + H_2O + [\alpha\text{-}SiW_{12}O_{40}]^{4-} \quad (3)$$

UV−visible spectra obtained by Toth and Anson suggested that a stable complex is formed between reduced iron-substituted poyoxometalates and NO.[8] Figure 3 shows that the transition of the RDE voltammogram from fully reductive (curve (a)) to fully oxidative (curve (b)) occurs in the potential region of process I during the course of bulk reductive electrolysis of $[\alpha\text{-}SiW_{12}O_{40}]^{4-}$ to $[\alpha\text{-}SiW_{12}O_{40}]^{5-}$ in both the presence and absence of NO_2^-. In the presence of NO_2^-, bulk electrolysis occurs via coupling of the $[\alpha\text{-}SiW_{12}O_{40}]^{4-} + e^- \rightarrow [\alpha\text{-}SiW_{12}O_{40}]^{5-}$ and reaction 3.

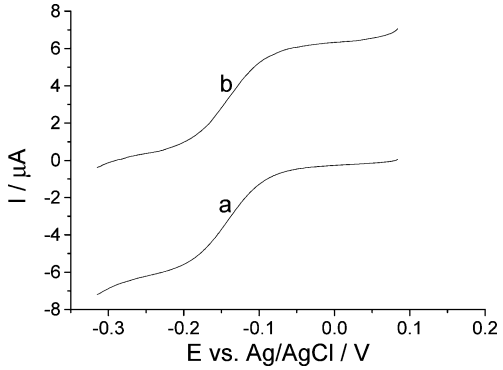

Figure 3. RDE voltammograms obtained (a) before and (b) after a one-electron reductive bulk electrolysis of 0.5 mM $[\alpha\text{-}SiW_{12}O_{40}]^{4-}$ (potential hold at ca. 0.3 V vs Ag/AgCl) in 1 M H_2SO_4 + 1 M Na_2SO_4 aqueous media. A scan rate of 10 mV s^{-1} and rotation rate of 500 rpm were used. An identical voltammetric result is obtained after bulk electrolysis when 5 mM NO_2^- is initially present.

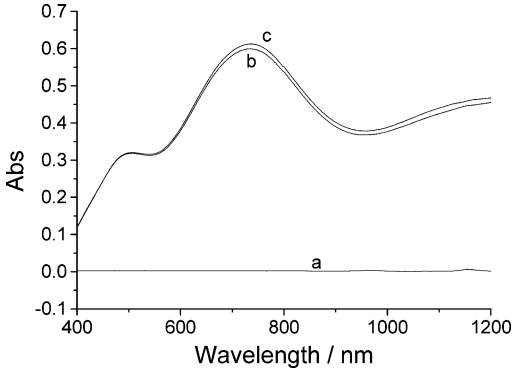

Figure 4. Electronic spectra obtained (a) before and (b) after exhaustive bulk reductive electrolysis of 0.5 mM $[\alpha\text{-}SiW_{12}O_{40}]^{4-}$ in 1 M H_2SO_4 + 1 M Na_2SO_4 in the absence (a and b) and presence (c) of 5 mM NO_2^-.

Thus, ultimately after all the NO_2^- is consumed, then $[\alpha\text{-}SiW_{12}O_{40}]^{4-}$ is reduced to $[\alpha\text{-}SiW_{12}O_{40}]^{5-}$. The reversible half-wave potential remains unchanged during the course of bulk electrolysis, even if the solution initially contains a large excess of NO_2^-. In contrast to the situations prevailing with iron-substituted polyoxometalate,[8] $[\alpha\text{-}SiW_{12}O_{40}]^{4-}$ may be completely reduced to $[\alpha\text{-}SiW_{12}O_{40}]^{5-}$ in either the presence or absence of NO_2^- and no stable complex is formed between $[\alpha\text{-}SiW_{12}O_{40}]^{5-}$ and NO.

Diffusion coefficients of 3.7×10^{-6} and 3.6×10^{-6} cm^2 s^{-1} were obtained for $[\alpha\text{-}SiW_{12}O_{40}]^{4-}$ and $[\alpha\text{-}SiW_{12}O_{40}]^{5-}$, respectively, using the Levich equation[22] and the RDE steady-state limiting current.

Electronic spectra of 0.5 mM $[\alpha\text{-}SiW_{12}O_{40}]^{5-}$ (Figure 4) in the presence and absence of NO (generated from the electrocatalytic reduction of HNO_2) also are essentially identical. This supports the inference made from the voltammetric experiments (Figure 3) that no stable complex is formed between $[\alpha\text{-}SiW_{12}O_{40}]^{5-}$ and NO. The stoichiometric form of the catalytic reaction scheme that can be proposed is represented by eqs 4 and 5.

$$[\alpha\text{-}SiW_{12}O_{40}]^{4-} + e^- \rightleftharpoons [\alpha\text{-}SiW_{12}O_{40}]^{5-} \quad (4)$$

$$H^+ + HNO_2 + [\alpha\text{-}SiW_{12}O_{40}]^{5-} \rightarrow NO + H_2O + [\alpha\text{-}SiW_{12}O_{40}]^{4-} \quad (5)$$

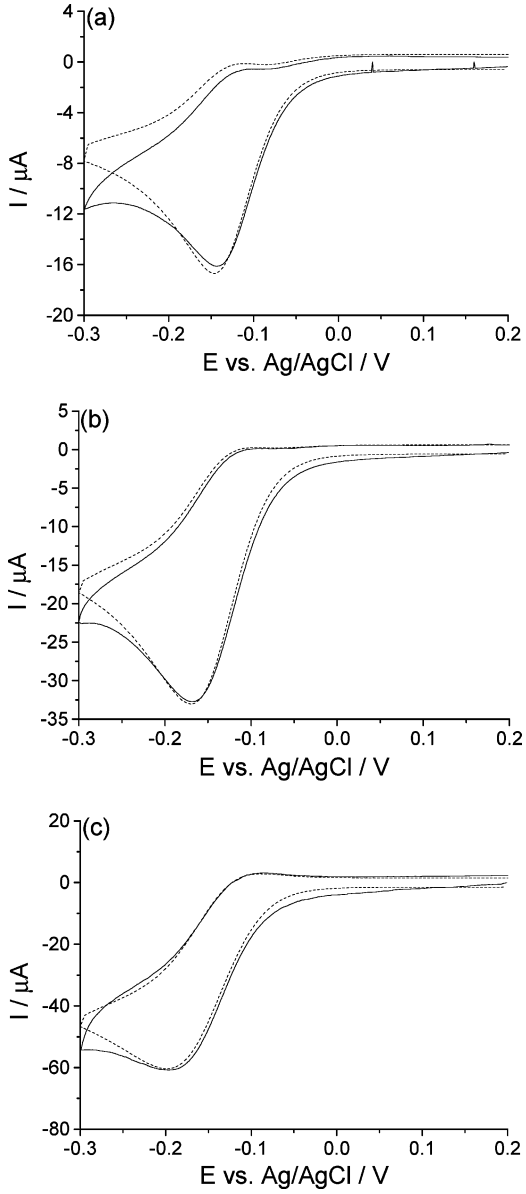

Figure 5. Comparison of experimental (—) cyclic voltammograms for the reduction of 0.9 mM of $[\alpha\text{-SiW}_{12}O_{40}]^{4-}$ in the presence of 1 mM NO_2^- in 1 M H_2SO_4 + 1 M Na_2SO_4 and simulated (- - -) data according to the mechanism described by eqs 4 and 5 with $k_f = 4 \times 10^4$ s^{-1} M^{-1}, $E^{0'}_{soln} = -0.144$ V, D ($[\alpha\text{-SiW}_{12}O_{40}]^{4-/5-}$) = 3.7×10^{-6} cm^2 s^{-1}, and D (HNO_2) = 2×10^{-5} cm^2 s^{-1}. Scan rates are (a) 0.02, (b) 0.1, and (c) 0.5 V s^{-1}.

1.4. Quantitative Analysis of Electrocatalytic Kinetics by Numerical Simulation of Cyclic Voltammetry. Nicholson and Shain[26] have developed a widely used voltammetric theory that provides a convenient analytical expression for kinetic analysis of electrocatalytic reactions under steady-state pseudo-first-order reaction conditions (substrate concentration is in a large excess compared to the electron-transfer mediator). Voltammograms relevant to this situation exhibit a sigmoidal rather than peaked shape and are characterized by a limiting current region. In the present case, the catalytic reaction is not operating under these conditions, as evidenced by the transient, scan-rate-dependent, peak-shaped rather than steady-state sigmoidal shaped voltammograms. Consequently, simulations rather than analytical solution are needed to model the reaction scheme.

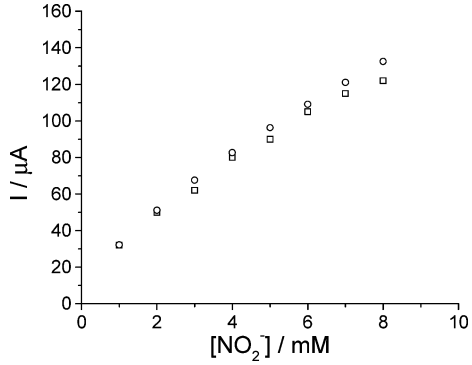

Figure 6. Comparison of experimental (□) and simulated (○) voltammetric peak currents obtained for reduction of 0.9 mM $[\alpha\text{-SiW}_{12}O_{40}]^{4-}$ in 1 M H_2SO_4 + 1 M Na_2SO_4 at a 3-mm-diameter GC electrode as a function of concentration of NO_2^- ($\upsilon = 0.1$ V s^{-1}).

From a mechanistic perspective, a trimolecular rate reaction (eq 5) is unlikely. Consequently, in initial numerical simulations, an initial guess was made that the bimolecular reaction between HNO_2 and $[\alpha\text{-SiW}_{12}O_{40}]^{5-}$ is rate limiting (rate constant of k_f). Of course, the hydrogen ion also may be present in a rate-limiting step. However, since H^+ is in a large excess, its concentration remains constant during the course of the voltammetric experiments and, if relevant, may be incorporated easily into analysis the reaction scheme as a constant. Simulated voltammograms obtained using a k_f value of 4×10^4 s^{-1} M^{-1} agree very well with experimental ones obtained in 1 M H_2SO_4 + 1 M Na_2SO_4 at scan rates of 0.02, 0.1, and 0.5 V s^{-1} (Figure 5). The dependence of the peak current on NO_2^- concentration for reduction of 0.9 mM $[\alpha\text{-SiW}_{12}O_{40}]^{4-}$ obtained experimentally and by simulation (Figure 6) also is consistent with a k_f value of 4×10^4 s^{-1} M^{-1}. However, in less acidic (0.1 M H_2SO_4 and 1 M Na_2SO_4) media where the $[H^+]$ decreases by an order of magnitude, the k_f value of 4×10^3 s^{-1} M^{-1} also has decreased by a factor of 10 (Figure 7). This implies that the catalytic reaction rate constant also exhibits a first-order dependence on the proton concentration. This k_f value in less acidic conditions also is consistent with the value of 3.73×10^3 s^{-1} M^{-1} obtained in aqueous 0.1 M H_2SO_4 at 17 °C by Dong and co-workers using steady-state voltammetry at a microdisk electrode under pseudo-first-order conditions.[11]

The β isomer also exhibits three analogous processes in acid conditions, but with $E^{0'}_{soln}$ values of −0.036, −0.159, and −0.401 V vs Ag/AgCl in 1 M H_2SO_4 + 1 M Na_2SO_4. Thus, the β form is easier to reduce than the α isomer, as reported in the literature.[1,27−29] Nitrite catalysis also was detected with the $[\beta\text{-SiW}_{12}O_{40}]^{4-}$ isomer (Figure 8). In this case, comparison of simulated and experimental voltammograms gives a slower bimolecular rate constant of 1.3×10^4 s^{-1} M^{-1} in 1 M H_2SO_4 + 1 M Na_2SO_4. Hence, $[\beta\text{-SiW}_{12}O_{40}]^{5-}$ is catalytically less active than the α form. Since the

(26) Nicholson, R. S.; Shain, I. *Anal. Chem.* **1964**, *36*, 706.
(27) Himeno, S.; Osakai, T.; Saito, A. *Bull. Chem. Soc. Jpn.* **1989**, *62*, 1335.
(28) Tézé, A.; Canny, J.; Gurban, L.; Thouvenot, R.; Hervé, G. *Inorg. Chem.* **1996**, *35*, 1001.
(29) Zhang, J.; Bond, A. M.; Richardt, P. J. S.; Wedd, A. G. *Inorg. Chem.* **2004**, *43*, 8263.

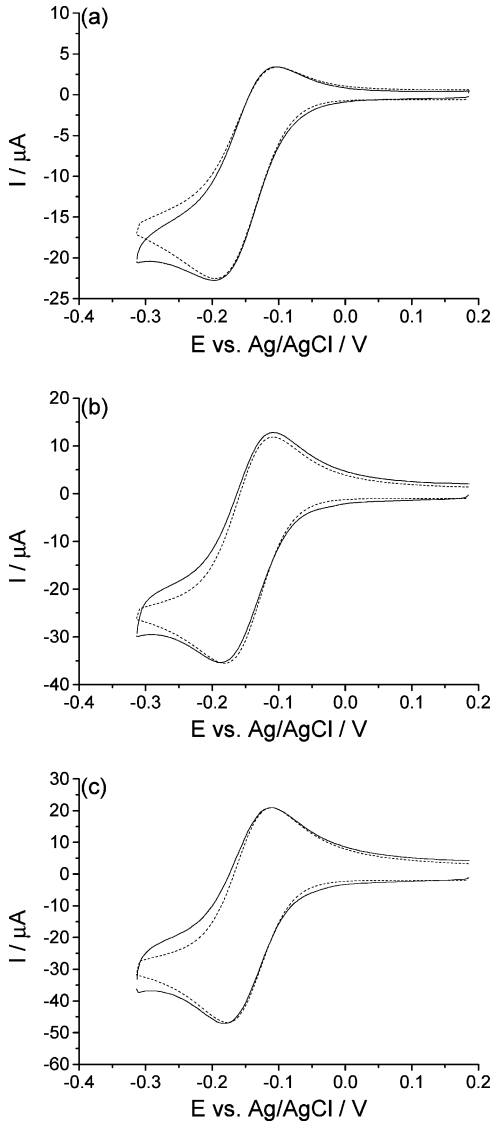

Figure 7. Comparison of experimental (—) cyclic voltammograms for the reduction of 1.1 mM of $[\alpha\text{-SiW}_{12}O_{40}]^{4-}$ in the presence of 0.9 mM NO_2^- in 0.1 M H_2SO_4 + 1 M Na_2SO_4 and simulated (- - -) data according to the mechanism described in eqs 4 and 5 with $k_f = 4 \times 10^3$ s^{-1} M^{-1}, $E^{0'}_{soln} = -0.144$ V, D ($[\alpha\text{-SiW}_{12}O_{40}]^{4-/5-}$) $= 3.7 \times 10^{-6}$ cm^2 s^{-1}, and D (HNO_2) $= 2 \times 10^{-5}$ cm^2 s^{-1}. Scan rates are (a) 0.1, (b) 0.5, and (c) 1 V s^{-1}.

reversible potentials for the $[\beta\text{-SiW}_{12}O_{40}]^{4-/5-}$ and $[\alpha\text{-SiW}_{12}O_{40}]^{4-/5-}$ couples are −0.036 and −0.144 V vs Ag/AgCl, respectively, in 1 M H_2SO_4 + 1 M Na_2SO_4, $[\beta\text{-SiW}_{12}O_{40}]^{5-}$ is a weaker reducing reagent than $[\alpha\text{-SiW}_{12}O_{40}]^{5-}$. If the rate-determining step involves an outer-sphere electron-transfer reaction, then on the basis of Marcus theory,[30,31] their similar sizes and not too different structures both the reorganization energy (determined by the sizes of reactants) and the precursor formation equilibrium constant (determined by the sizes and charge of the reactants) for the α and β isomers of $[SiW_{12}O_{40}]^{5-}$ are predicted to be similar. In this case, the slower rate constant for the β isomer

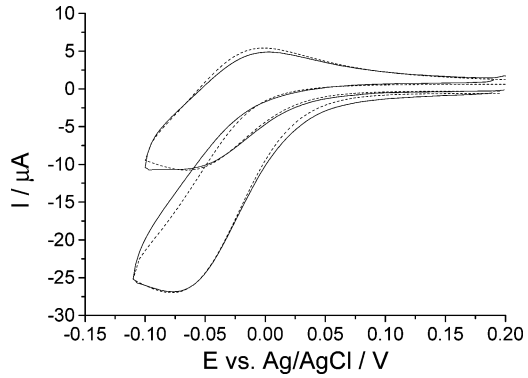

Figure 8. Comparison of experimental (—) cyclic voltammograms for the reduction of 0.9 mM of $[\beta\text{-SiW}_{12}O_{40}]^{4-}$ in the presence (lower curve) and absence (upper curve) of 1 mM NO_2^- in 1 M H_2SO_4 + 1 M Na_2SO_4 and simulated (- - -) data according to the mechanism described by eqs 4 and 5 with $k_f = 1.3 \times 10^4$ s^{-1} M^{-1}, $E^{0'}_{soln} = -0.036$ V, D ($[\beta\text{-SiW}_{12}O_{40}]^{4-/5-}$) $= 3.7 \times 10^{-6}$ cm^2 s^{-1}, and D (HNO_2) $= 2 \times 10^{-5}$ cm^2 s^{-1}. ($v = 0.1$ V s^{-1}).

may be a direct consequence of the smaller driving force available for the β isomer.

1.5. Details of Catalytic Mechanism. On the basis of the kinetic data, a mechanism involving reactions 6−8 is proposed for nitrite reduction catalyzed by $[SiW_{12}O_{40}]^{5-}$ in acidic media

$$[SiW_{12}O_{40}]^{4-} + e^- \rightleftharpoons [SiW_{12}O_{40}]^{5-} \quad (6)$$

$$H^+ + HNO_2 \overset{K}{\rightleftharpoons} NO^+ + H_2O \quad (7)$$

$$NO^+ + [SiW_{12}O_{40}]^{5-} \xrightarrow{k_{f1}} NO + [SiW_{12}O_{40}]^{4-} \quad (8)$$

where K is the (concentration based) equilibrium constant for reaction 7 and k_{f1} is the bimolecular reaction rate constant for what is likely to be an outer-sphere process. Reaction 7 has been reported to be a rapid reversible process.[25] Consequently,

$$[NO^+] = K[H^+][HNO_2] \quad (9)$$

Since $[H^+]$ in the 0.1 or 1 M H_2SO_4 aqueous media is in a large excess, it may be regarded as a constant, so that

$$[NO^+] = K_1[HNO_2] \quad (10)$$

where $K_1 = K[H^+]$.

According to the postulated mechanism

$$\text{Rate} = k_{f1}[NO^+][[SiW_{12}O_{40}]^{5-}] \quad (11)$$

which after substitution via eq 10 gives,

$$\text{Rate} = k_{f1}K_1[HNO_2][[SiW_{12}O_{40}]^{5-}] \quad (12)$$

which is first order in both HNO_2 and $[SiW_{12}O_{40}]^{5-}$, as deduced from comparison of experimental and simulated voltammograms. According to this mechanism, the votammetrically determined rate constant, k_f, is equal to $k_{f1}K_1$ (or $k_{f1}K[H^+]$), which explains the observed first order

(30) Eberson, L. *Electron-Transfer Reaction in Organic Chemistry*; Springer-Verlag: Berlin, 1987.
(31) Bard, A. J.; Faulkner, L. R. *Electrochemical Methods: Fundamentals and Applications*; Wiley: New York, 2001.

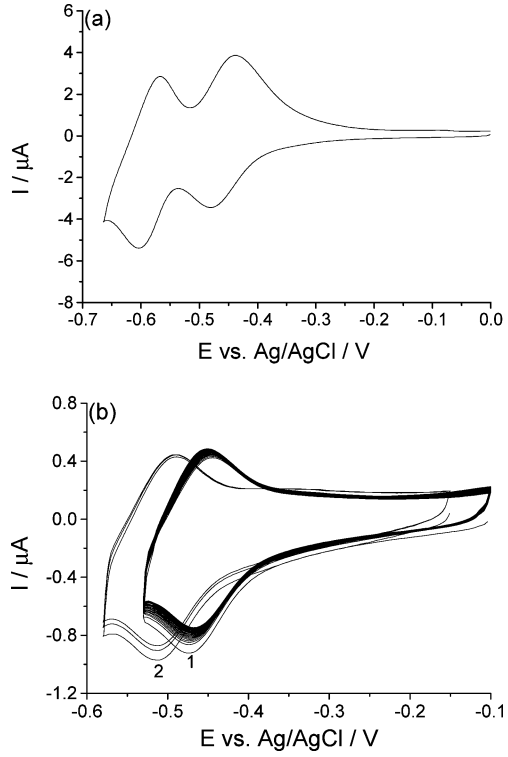

Figure 9. Cyclic voltammograms obtained when a 3-mm-diameter GC electrode modified with (a) a thick film of $[Ru(bipy)_3]_2[\alpha\text{-}SiW_{12}O_{40}]$ prior to being placed in contact with 1 M H_2SO_4 solution (b) a thin film of $[Ru(bipy)_3]_2[\alpha\text{-}SiW_{12}O_{40}]$ prior to being placed in contact with 1 M H_2SO_4 solution (30 cycles of potential) (curve 1) and 0.1 M H_2SO_4 solution (3 cycles of potential) (curve 2). $\upsilon = 0.05$ V s^{-1}.

dependence of k_f on $[H^+]$, as well as on $[HNO_2]$ and $[SiW_{12}O_{40}]$.$^{5-}$

2. Solid-State Voltammetry of $[Ru(bipy)_3]_2[\alpha\text{-}SiW_{12}O_{40}]$.

2.1. $[Ru(bipy)_3]_2[\alpha\text{-}SiW_{12}O_{40}]$ Modified GC Electrode. A $[Bu_4N]_4[\alpha\text{-}SiW_{12}O_{40}]$-modified electrode in contact with aqueous H_2SO_4 electrolyte is unstable due to rapid dissolution of solid. However, a modified electrode based on $[Ru(bipy)_3]_2[\alpha\text{-}SiW_{12}O_{40}]$ is much more stable as this material and its reduced forms exhibits low solubility in aqueous H_2SO_4 media.

Figure 9a shows a voltammogram of a $[Ru(bipy)_3]_2$-$[\alpha\text{-}SiW_{12}O_{40}]$-modified electrode in 1 M H_2SO_4 solution (1 mM $[Bu_4N]_4[\alpha\text{-}SiW_{12}O_{40}]$ solution was used to prepare the modified electrode). Two processes are detected within the potential window range available, and both remain fairly stable upon extended periods of cycling of the potential. The $E^{0'}_{solid}$ values of -0.457 and -0.585 V vs Ag/AgCl, respectively, obtained from the average of the reduction and oxidation peak potentials, occur at a much more negative potential than their $E^{0'}_{soln}$ solution-phase $[\alpha\text{-}SiW_{12}O_{40}]^{4-/5-}$ and $[\alpha\text{-}SiW_{12}O_{40}]^{5-/6-}$ counterparts (see Figure 1).

The peak-to-peak separations of 0.042 and 0.038 V for the first and the second processes, respectively, at a scan rate of 0.05 V s^{-1} are larger than the theoretical value of 0 V predicted for an ideal reversible surface-confined thin-film process.[31] This is partially attributable to the fact that a thick rather than thin film or an array of microcrystals is present on this electrode surface, so that the voltammetry is influenced by diffusion within the solid.

Thin-film-type behavior simplifies the theoretical interpretation of the voltammetry. The concentration of $[\alpha\text{-}SiW_{12}O_{40}]^{4-}$ present in the CH_3CN solution used to prepare the $[Ru(bipy)_3]_2[\alpha\text{-}SiW_{12}O_{40}]$-modified GC electrodes was found to determine the voltammetric behavior. Experiments with variable concentrations revealed that use of 0.4 mM $[\alpha\text{-}SiW_{12}O_{40}]^{4-}$ produced close to ideal thin-film voltammetry for the $[\alpha\text{-}SiW_{12}O_{40}]^{4-/5-}$ process even after extended periods of cycling of the potential (Figure 9b). Integration of background-subtracted current−time curve at a scan rate of 0.05 V s^{-1} equates to a total surface coverage of 9×10^{-12} mol of electrochemically active $[\alpha\text{-}SiW_{12}O_{40}]^{4-}$ or a surface coverage of 1.3×10^{-10} mol cm^{-2} for a 3-mm-diameter electrode. Under these conditions, a smaller peak current was measured versus the thicker film case and the peak-to-peak separation of 0.022 V is closer to the theoretical value of 0 V predicted for a reversible surface confined thin film process. The $E^{0'}_{solid}$ value of -0.457 V vs Ag/AgCl is independent of film thickness. The slow decay of the current during the cycling of potential is attributed to the small-level dissolution of microcrystals.

Comparison of cyclic voltammograms obtained for a $[Ru(bipy)_3]_2[\alpha\text{-}SiW_{12}O_{40}]$-modified GC electrode in 1.0 and 0.1 M H_2SO_4 (Figure 9b) shows that the $E^{0'}_{solid}$ shifts by 0.04 V in the negative direction upon a 10-fold decrease of sulfuric acid concentration. In contrast, the $E^{0'}_{soln}$ value for the fully solution-phase $[\alpha\text{-}SiW_{12}O_{40}]^{4-/5-}$ process is almost independent of acid concentration (Figure 1b). This difference arises from the fact that the one-electron reduction detected at a $[Ru(bipy)_3]_2[\alpha\text{-}SiW_{12}O_{40}]$-modified electrode involves a solid-state component that requires insertion of H^+ into the reduced form of the solid in order to provide the necessary charge neutralization process (eq 13).

$$[Ru(bipy)_3]_2[\alpha\text{-}SiW_{12}O_{40}](solid) + H^+(soln) + e^- \rightleftharpoons H[Ru(bipy)_3]_2[\alpha\text{-}SiW_{12}O_{40}](solid) \quad (13)$$

The proton, originally in solution phase, could be incorporated into the well-organized $[\alpha\text{-}SiW_{12}O_{40}]^{5-}$ crystal structure via binding to an oxygen site or simply be present as a charge-balancing cation in the crystal lattice. This process leads to a decrease in entropy (less-chaotic state) and this may contribute to the reversible potential of $[\alpha\text{-}SiW_{12}O_{40}]^{4-/5-}$ process in the three-dimensional solid state being more negative than that in the two-dimensional thin-layer state[32] and also in the dissolved state (see Figure 1).

If eq 13 is reversible, then the relevant Nernst relationship may be written as

$$E = E^{0'}_{solid1} + \frac{RT}{F} \ln \frac{a_{Ox(solid)}\, a_{H^+}(soln)}{a_{Red(solid)}} \quad (14)$$

where the reversible potential $E^{0'}_{solid1}$ includes contributions from both electron transfer and H^+ transfer between water and the microcrystal. In eq 14, $a_{Red(solid)}$ and $a_{Ox(solid)}$ are the activities of $H[Ru(bipy)_3]_2[\alpha\text{-}SiW_{12}O_{40}](solid)$ and

(32) Liu, S.; Shi, Z.; Dong, S. *Electroanalysis* **1998**, *10*, 891.

$[Ru(bipy)_3]_2[\alpha\text{-}SiW_{12}O_{40}]$(solid), respectively. a_{H^+} (soln) represents the activity of H^+. Under conditions where the concentration of H^+ is very high, then the a_{H^+} (soln) is essentially constant during the course of voltammetric experiment. Consequently, eq 14 can be rewritten as

$$E = E^{0\prime}_{solid} + \frac{RT}{F}\ln\frac{a_{Ox(solid)}}{a_{Red(solid)}} \quad (15)$$

where

$$E^{0\prime}_{solid} = E^{0\prime}_{solid1} + \frac{RT}{F}\ln a_{H^+(soln)}$$

is the apparent reversible potential measured experimentally and is expected to be pH dependent. Since the activity coefficients of H^+ in 0.1 and 1 M H_2SO_4 are 0.316 and 0.158, respectively,[33] a negative reversible potential shift of 0.041 V is expected when the concentration of H_2SO_4 is decreased from 1 to 0.1 M (assuming $[H^+]$ also is decreased by a factor of 10), which agrees well with the experimentally observed value.

Voltammograms for the solid form of the $[\alpha\text{-}SiW_{12}O_{40}]^{4-/5-}$ process can be reversible in acidic conditions because the transfer of a mobile proton between the solution and bulk solid phases required for charge neutralization purpose can be rapid.[34] In contrast, in the presence of 0.2 M Na_2SO_4 electrolyte solution (no acid present), an ill-defined voltammogram with a much smaller peak current was obtained. Presumably, the incorporation of Na^+ into $[Ru(bipy)_3]_2[\alpha\text{-}SiW_{12}O_{40}]$(solid) is more difficult. Oxidation of $[Ru(bipy)_3]^{2+}$ to $[Ru(bipy)_3]^{3+}$ also could be expected at a $[Ru(bipy)_3]_2[\alpha\text{-}SiW_{12}O_{40}]$(solid) chemically modified electrode. However, transfer of HSO_4^- or SO_4^{2-} from solution to give $[Ru(bipy)_3]_2[\alpha\text{-}SiW_{12}O_{40}][HSO_4]_2$(solid) or $[Ru(bipy)_3]_2[\alpha\text{-}SiW_{12}O_{40}]_2[SO_4]$(solid) is required in this case to achieve charge neutralization. Apparently, this is not such a favorable process, as only a drawn-out ill-defined voltammogram is detected at positive potentials for oxidation of a $[Ru(bipy)_3]_2[\alpha\text{-}SiW_{12}O_{40}]$(solid) chemically modified electrode (voltammogram not shown).

Interestingly, an electrocatalytic response is still detected in the presence of NO_2^- at the $[Ru(bipy)_3]_2[\alpha\text{-}SiW_{12}O_{40}]$(solid) chemically modified electrode (Figure 10) when the potential is scanned in the region of $[\alpha\text{-}SiW_{12}O_{40}]^{4-/5-}$ process. A catalytic process in this instance could arise from the overall reaction

$$H[Ru(bipy)_3]_2[\alpha\text{-}SiW_{12}O_{40}](solid) + HNO_2(soln) \rightarrow [Ru(bipy)_3]_2[\alpha\text{-}SiW_{12}O_{40}](solid) + H_2O + NO \quad (16)$$

However, a sizable current is detected well before the onset of the solid-state redox couple, even though the maximum value is found near the peak position for this process. The current detected at less-negative potentials could be due to a contribution from reaction between a low concentration

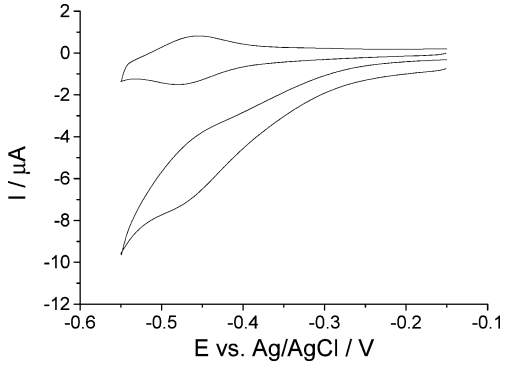

Figure 10. Cyclic voltammograms obtained when a $[Ru(bipy)_3]_2[\alpha\text{-}SiW_{12}O_{40}]$ thin-film-modified GC electrode (3 mm diameter) is immersed in 1 M H_2SO_4 solution in the absence (upper curve) and presence (lower curve) of 1 mM NO_2^-. $\upsilon = 0.05$ V s^{-1}.

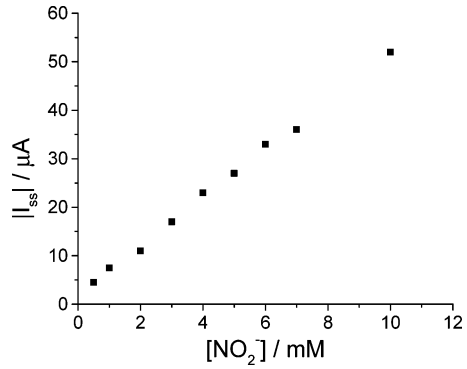

Figure 11. Catalytic current obtained at a potential of −0.53 V vs Ag/AgCl when a thin-film $[Ru(bipy)_3]_2[\alpha\text{-}SiW_{12}O_{40}]$ chemically modified GC electrode in contact with 1 M H_2SO_4 is reduced in the presence of NO_2^-. $\upsilon = 0.05$ V s^{-1}.

of dissolved $[\alpha\text{-}SiW_{12}O_{40}]^{5-}$ (generated from either dissolved $[\alpha\text{-}SiW_{12}O_{40}]^{4-}$ or the dissolution of reduced solid) and NO_2^-.

2.2. Dependence on Concentration of NO_2^-, $[Ru(bipy)_3]^{2+}$, and H^+. Figure 11 provides a plot of the catalytic current (I_{cat}, measured at $E = -0.53$ V vs Ag/AgCl) versus $[NO_2^-]$ obtained when a $[Ru(bipy)_3]_2[\alpha\text{-}SiW_{12}O_{40}]$-modified GC electrode is in contact with 1 M H_2SO_4. The slope obtained by linear fitting of the data is 5.0 mA M^{-1}. The fact that the magnitude of the catalytic current only decreases slightly (ca. 10%) on addition of 0.1 mM dissolved $[Ru(bipy)_3]^{2+}$ to a solution containing 1 M H_2SO_4 suggests that a heterogeneous reaction pathway rather than a homogeneous reaction pathway involving the reaction between the $[\alpha\text{-}SiW_{12}O_{40}]^{5-}$ (generated from solid dissolution) and nitrite is predominant. Based on the analogy with the solution phase catalytic scheme, the simplest possible mechanism involving the chemically modified electrode case should be

$$[Ru(bipy)_3]_2[\alpha\text{-}SiW_{12}O_{40}](solid) + H^+(soln) + e^- \rightleftarrows H[Ru(bipy)_3]_2[\alpha\text{-}SiW_{12}O_{40}](solid) \quad (17)$$

$$H^+(soln) + HNO_2(soln) \overset{K}{\rightleftarrows} NO^+(soln) + H_2O(soln) \quad (18)$$

$$NO^+(soln) + H[Ru(bipy)_3]_2[\alpha\text{-}SiW_{12}O_{40}](solid) \xrightarrow{k_{f2}} NO + [Ru(bipy)_3]_2[\alpha\text{-}SiW_{12}O_{40}](solid) + H^+(soln) \quad (19)$$

(33) Iobo, V. M. M. *Handbook of Electrolyte Solutions*; Elsevier: New York, 1989.
(34) Kulesza, P. J.; Faulkner, L. R.; Chen, J.; Klemperer, W. G. *J. Am. Chem. Soc.* **1991**, *113*, 379.

This scheme could be postulated to give

$$\text{Rate of } H[Ru(bipy)_3]_2[\alpha\text{-}SiW_{12}O_{40}] \text{ consumption} = k_{f2}[NO^+]\Gamma_{Red} = k_{f2}K[H^+][HNO_2]\Gamma_{Red} \quad (20)$$

where k_{f2} is the rate constant of the heterogeneous bimolecular catalytic reaction (with the units of s^{-1} M^{-1}) and Γ_{Red} is the potential-dependent surface concentration of $H[Ru(bipy)_3]_2[\alpha\text{-}SiW_{12}O_{40}]$(solid) (units of mol cm^{-2}). However, in the case of the chemically modified electrode, the catalytic current is independent of $[H^+]$ for experiments undertaken with sulfuric acid concentrations of 1.0, 0.10, and 0.02 M at the level of uncertainty of 5%. This is in stark contrast to the first-order dependence of $[H^+]$ found with dissolved electroactive reactants and products (see above). This difference may be associated with the fact that the reversible potential of the solid-state process (eq 17), hence k_{f2}, is also pH dependent, which may modify the influence of the pH on the rate constant for the catalytic reaction. Clearly, the mechanism is more complex and probably significantly different from a reaction scheme based on direct analogy with the dissolved $[SiW_{12}O_{40}]^{4-/5-}$ case. Given that uncertainty also exists in the details of chemically modified electrode mechanism because of a small level of solubility of the solids and also with respect to the activities that should be used in the theoretical analysis for the solids, further speculation on the mechanism is not warranted.

Conclusion

A reversible, almost pH-independent, one-electron $[SiW_{12}O_{40}]^{4-/5-}$ reduction process is detected voltammetrically in acidic conditions for dissolved α and β isomers of $[SiW_{12}O_{40}]^{4-}$. A reversible one-electron reduction process also is found with surface-confined $[Ru(bipy)_3]_2[\alpha\text{-}SiW_{12}O_{40}]$. However, for this solid-state case, the process is defined by the reaction, $[Ru(bipy)_3]_2[\alpha\text{-}SiW_{12}O_{40}](solid) + H^+(soln) + e^- \rightarrow H[Ru(bipy)_3]_2[\alpha\text{-}SiW_{12}O_{40}](solid)$, and so a pH dependence is introduced that is not found with the dissolved $[SiW_{12}O_{40}]^{4-/5-}$ case. The voltammetry in acid media for both solution-phase forms and the solid-state form of the polyoxometalate exhibits an electrocatalytic response in the presence of NO_2^-. The dissolved form of $[\alpha\text{-}SiW_{12}O_{40}]^{5-}$ is found to be more catalytically active with respect to reduction of HNO_2 than the β isomer. A mechanism for the fully solution-phase catalytic reaction scheme postulated on the basis of spectroelectrochemical results and kinetic data obtained from voltammetric experiments exhibits a first-order dependence on $[HNO_2]$, $[H^+]$, and reduced polyoxometalate. The detailed mechanism for the chemically modified electrode situation is unknown but appears to be significantly more complex than that postulated on the basis of analogy with the solution-soluble $[SiW_{12}O_{40}]^{4-/5-}$ case.

The iron-substituted polyoxometalates studied by Toth and Anson[8] exhibit significant catalytic activity toward nitrite reduction at much higher pH (where nitrite is unstable) than is the case with the $[SiW_{12}O_{40}]^{4-}$ system. Since a wide range of unsubstituted polyoxometalates have been successfully synthesized,[1,6] it may be expected that some of these would have higher catalytic activity for nitrite reduction at higher pH values than is the case with $[SiW_{12}O_{40}]^{4-}$. In fact, recent work by McCormac and co-workers has shown that a significant catalytic current was obtained at pH 4.5 when a multilayer $[Fe(bipy)_3]_3[P_2W_{18}O_{62}]$-modified electrode was used for nitrite reduction.[14a]

Acknowledgment. The authors thank the Australian Research Council for financial support and Dr. Sixuan Guo for conducting some of the experiments. Prof. A. G. Wedd (University of Melbourne) and his research group are also gratefully acknowledged for supplying the α and β isomers of $K_4[SiW_{12}O_{40}]$ and $[Bu_4N]_4[\alpha\text{-}SiW_{12}O_{40}]$ used in these studies.

IC0519943